ISSN 1063-7761, Journal of Experimental and Theoretical Physics, 2013, Vol. 117, No. 5, pp. 879–884. © Pleiades Publishing, Inc., 2013.
Original Russian Text © A.M. Vorotynov, G.M. Abramova, A.I. Pankrats, G.A. Petrakovskii, S.M. Zharkov, G.M. Zeer, V.I. Tugarinov, M.V. Rautskii, V.V. Sokolov, 2013, published in Zhurnal Eksperimental'noi i Teoreticheskoi Fiziki, 2013, Vol. 144, No. 5, pp. 1009–1015.

ORDER, DISORDER, AND PHASE TRANSITION IN CONDENSED SYSTEM

Magnetic Resonance in a Cu–Cr–S Structure

A. M. Vorotynov[a,*], G. M. Abramova[a], A. I. Pankrats[a,b], G. A. Petrakovskii[a], S. M. Zharkov[a,b], G. M. Zeer[b], V. I. Tugarinov[a], M. V. Rautskii[a], and V. V. Sokolov[c]

[a] *Kirensky Institute of Physics, Siberian Branch, Russian Academy of Sciences, Krasnoyarsk, 660036 Russia*
[b] *Siberian Federal University, Krasnoyarsk, 660041 Russia*
[c] *Nikolaev Institute of Inorganic Chemistry, Siberian Branch, Russian Academy of Sciences, Novosibirsk, 630090 Russia*
**e-mail: sasa@iph.krasn.ru*

Received April 29, 2013

Abstract—A layered Cu–Cr–S structure composed of single-crystal $CuCrS_2$ layers and thin $CuCr_2S_4$ plates embedded in them has been investigated by the magnetic resonance and scanning electron microscopy methods. The Curie temperature and saturation magnetization of the spinel phase of the investigated samples have been determined. The thickness of the $CuCr_2S_4$ layers has been estimated. The dependence of the grown-crystal topology on synthesis conditions has been established. An interpretation of the anomalous behavior of the magnetostatic oscillation intensity is offered.

DOI: 10.1134/S1063776113130189

1. INTRODUCTION

The search for and investigation of new materials with special magnetic and electric properties are among the priority directions of development of magnetism and solid-state physics. The experimental results accumulated to date lead to the conclusion that the interrelation of magnetic and electric properties is most pronounced in "layered" structures that are an alternation of anion and cation planes. Such a crystalline structure is characteristic of 3*d*-metal monosulfides and disulfides [1, 2].

Layered copper–chromium disulfide ($CuCrS_2$) is known to be an antiferromagnet with a Neel temperature $T_N = 40$ K that has an alignment of magnetic moments similar to manganites, europium and manganese chalcogenides. The rhombohedral lattice of copper–chromium disulfide (structural type α-$NaFeO_2$) is a derivative of the NaCl structure and has space group $R3m$ [3]. Particular interest in $CuCrS_2$ stems from the fact that this compound belongs to layered intercalated materials, in which the weak (Van der Waals) bond, along with the ion–covalent bonds, plays an important role [1, 3]. The $CuCrS_2$ compound is considered [4] as a quasi-two-dimensional antiferromagnet whose magnetic properties are determined by the ferromagnetic alignment of the magnetic moments of trivalent chromium ions in the alternating triple CrS_2 layers and by their antiferromagnetic alignment between the CrS_2–Cu–CrS_2 layers. As further studies showed [5], the magnetic structure of $CuCrS_2$ turned out to be more complex than was assumed in the first works.

$CuCrS_2$ is a paramagnetic electron–ion semiconductor at room temperature and undergoes a superionic conductor–semiconductor transition at 670 K [6], an electronic transition at 110 K [7], and a transition to an antiferromagnetic state at 37 K [8, 9].

Quasi-two-dimensional layered structures that are three-dimensional crystals with a strong anisotropy of chemical bonds can be promising matrices for the production of new multilayered materials. Multilayered (magnetic/nonmagnetic, insulator/metal) structures can be produced by using various crystal growth technologies. Previously [10], it has been established that the physical properties of copper–chromium disulfide depend significantly on the sample preparation technology. In particular, the polycrystalline samples are single-phase ones and have a rhombohedral structure typical of $CuCrS_2$, while the single crystals [11] can contain an additional spinel phase ($CuCr_2S_4$).

In this paper, we present the results of our study of the magnetic resonance for samples composed of single-crystal $CuCrS_2$ layers (planes) and thin $CuCr_2S_4$ plates.

2. SAMPLE PREPARATION AND CHARACTERISTICS

Single crystals were synthesized from a polycrystalline $CuCrS_2$ powder whose X-ray diffractogram is presented in Fig. 1 in comparison with the X-ray diffractogram from the structural data bank.

The crystalline structure of polycrystals corresponds to the published data for $CuCrS_2$. The rhombohedral lattice parameters (space group $R3m$) are $a =$ 3.485 Å and $c = 18.70$ Å. No accompanying phases were detected within the error limits of the method.

We used the method of chemical transport reactions to grow $CuCrS_2$ single crystals and iodine as a

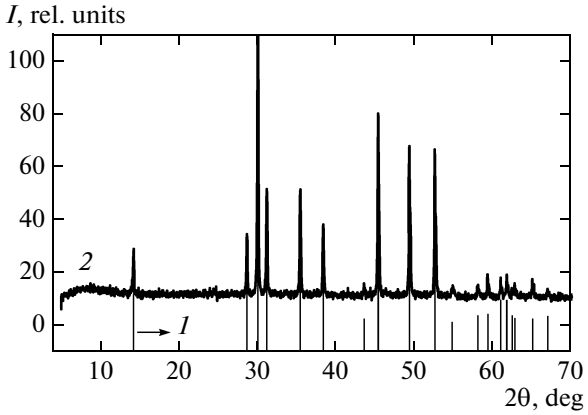

Fig. 1. X-ray diffractograms for polycrystalline copper–chromium disulfide at 300 K: the tabulated (*1*) and (*2*) experimental data.

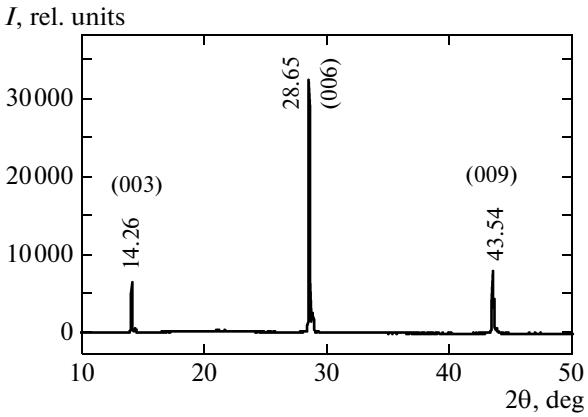

Fig. 2. X-ray diffractogram for a copper–chromium disulfide single-crystal plate at 300 K.

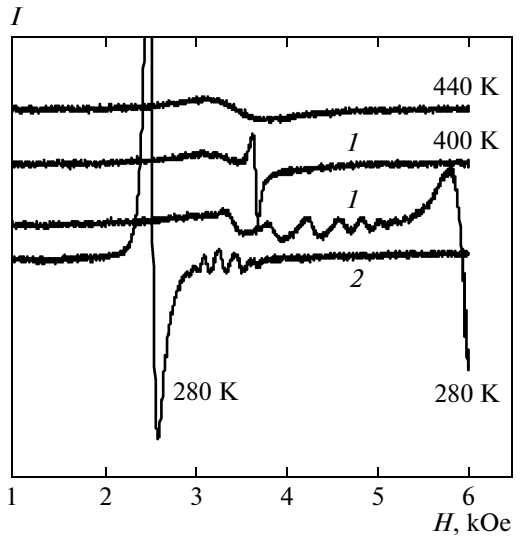

Fig. 3. Temperature evolution of the magnetic resonance spectra. Spectra *1* and *2* correspond to orientations of the external magnetic field perpendicular and parallel to the plane of the sample plate, respectively.

carrier. The synthesis was accomplished from a presynthesized polycrystalline $CuCrS_2$ powder that was loaded into a quartz ampoule; a temperature gradient was created along the ampoule. The geometrical sizes of the ampoules are: 20 mm in diameter, 160–180 mm in length, and 50–56 cm^3 in volume. The copper–chromium disulfide powder load was about 1 g. The iodine concentration in various experiments changed within the range 1.5–7 mg cm^{-3}. The temperature of the hot zone was 1050°C; the cold end of the ampoule was in the furnace zone at 750–800°C. We carried out five experiments, each with a process duration of at least 30 days. Thin plate-like crystals up to 5–10 mm in diameter and about 0.2 mm in thickness were grown.

Figure 2 shows the X-ray diffractogram measured on a copper–chromium disulfide single-crystal plate. The X-ray diffractogram exhibits lines that are characteristic of the rhombohedral structure of $CuCrS_2$ and that lead to the conclusion that the crystal growth plane corresponds to the (001) plane. This is consistent with the previously published data [11]. No iodine phases were detected. In contrast to the data from [11], in the crystals grown by the described method, no reflexes of the spinel phase were detected in the X-ray diffractograms obtained from the single-crystal plate surface. However, on the powders prepared by grinding the grown single-crystal plates, the X-ray diffractogram additionally exhibited one line (reflection (110)) that could be attributed to the spinel phase, just as in [11]. The absence of lines belonging to the spinel phase in the X-ray diffractogram obtained from the single-crystal plate surface can be explained by the absence of the spinel phase both on and near the plate surface.

3. EXPERIMENTAL RESULTS AND THEIR DISCUSSION

The magnetic resonance spectra were taken with a Bruker Elexsys E580 spectrometer operating in the X-band at temperatures 100 K $\leq T \leq$ 440 K. The temperature and angular dependences of the line width and the resonance field were investigated.

The temperature evolution of the magnetic resonance spectra is shown in Fig. 3. At temperatures above 420 K, a single line of Lorentzian shape with parameters $H_{res} = 3430$ Oe, $g = 1.99$, and $\Delta H = 690$ Oe corresponding to the paramagnetic resonance in the sample is observed in the paramagnetic phase. The line width (Fig. 4), about 700 Oe at $T = 440$ K, increases with decreasing temperature owing to the growth of critical fluctuations. Concurrently, the appearance of a second line ($\Delta H = 70$ Oe) corresponding to the ferromagnetic resonance of the $CuCrS_2$ phase is observed [9]. As the temperature decreases further, the width of this line increases only slightly. Additional magnetostatic oscillation modes appear at temperatures $T <$ 370 K (Fig. 3). They manifest themselves as oscilla-

tions on the wings of the main ferromagnetic resonance on the left or the right, depending on the orientation of the external magnetic field.

Such magnetostatic oscillations were observed previously in the ferromagnetic $HgCr_2S_4$ compound [12], where the sample was a thin disk.

The temperature dependence of the resonance fields for the observed lines is shown in Fig. 5. The upper (open circles) and lower (filled circles) curves in Fig. 5 correspond to the resonance fields of the main signal from the ferromagnetic phase for orientations of the external magnetic field perpendicular and parallel to the plane of the sample plate. The changes in the resonance field of the main signal are caused by an increase in the demagnetizing fields with decreasing temperature and are well described by the expressions for taking into account the demagnetizing fields in a thin ferromagnetic plate [13]:

$$\omega_0/\gamma = \sqrt{H_{res\parallel}(H_{res\parallel} + 4\pi M_0)}, \quad \omega_0/\gamma = H_{res\perp} - 4\pi M_0, \tag{1}$$

where ω_0 is the microwave emission frequency, γ is the gyromagnetic ratio, $H_{res\parallel,\perp}$ are the resonance fields for the corresponding magnetic field orientations, and $M_0 = 420$ G is the saturation magnetization extrapolated to $T = 0$ K. According to the magnetization measurements in [14], $M_0 = 365$ G. The points located between the upper and lower curves in Fig. 5 correspond to the positions of the magnetostatic modes for orientations of the external magnetic field perpendicular (open circles) and parallel (filled circles) to the plane of the sample plate. At a fixed frequency, the range of resonance fields for the magnetostatic oscillations in this case is equal to that predicted theoretically for thin plates [13]:

$$\sqrt{\left(\frac{\omega_0}{\gamma}\right)^2 + (2\pi M_0)^2} - 2\pi M_0 \le H \le \frac{\omega_0}{\gamma}, \quad \omega_0/\gamma \le H \le \omega_0/\gamma + 4\pi M_0 \tag{2}$$

for the parallel and perpendicular orientations, respectively. When the external magnetic field was rotated in the sample plane, no angular dependences of the main and magnetostatic signals were detected.

To ascertain whether $CuCr_2S_4$ in the form of thin ferromagnetic plates with finite sizes could exist in the sample, we investigated the microstructure and phase composition of our single-crystal samples (from different synthesis sets) by the scanning electron microscopy and energy dispersive X-ray spectroscopy methods on a JEOL JSM-7001F scanning electron microscope. An elemental analysis of the samples was performed on the end of the single-crystal plate along a line perpendicular to its plane. An example of an electron microscope image for the plate end is shown in Fig. 6. The visible layers in the figure belong to the $CuCrS_2$ phase and are determined by the crystal growth specificity.

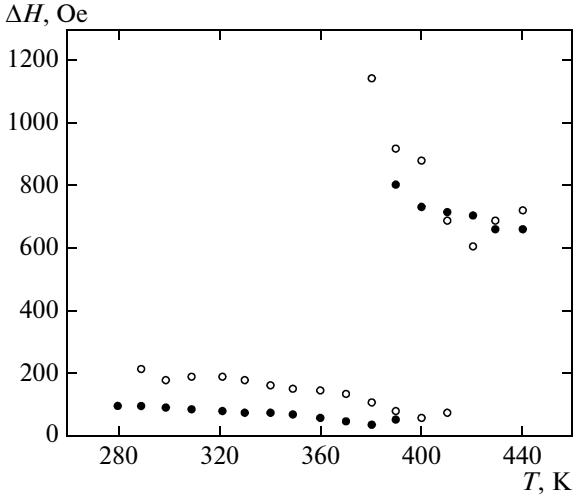

Fig. 4. Temperature dependence of the width of the main magnetic resonance line in the investigated sample. The open and filled circles correspond to orientations of the external magnetic field perpendicular and parallel to the plane of the sample plate, respectively.

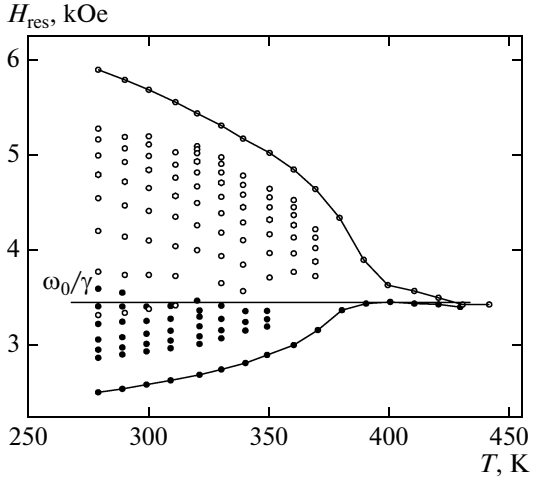

Fig. 5. Temperature dependence of the resonance fields for the main ferromagnetic resonance line (solid curves) and magnetostatic modes for different orientations of the external magnetic field (see the text).

Our analysis showed the following mean composition: S—40 at %, Cr—24 at %, and Cu—27 at %. The standard deviations in our analysis at various points of the sample are 1–2 at %.

We compared our data with chemical composition data typical of copper–chromium disulfide $CuCrS_2$ (Cu—25 at %, Cr—25 at %, S—50 at %) and spinel $CuCr_2S_4$ (Cu—14.3 at %, Cr—28.6 at %, S—57.1 at %).

It should be noted that we detected no regions with an elemental composition close to that of spinel $CuCr_2S_4$ in the investigated sample regions. This can be explained if we assume that the thickness of the

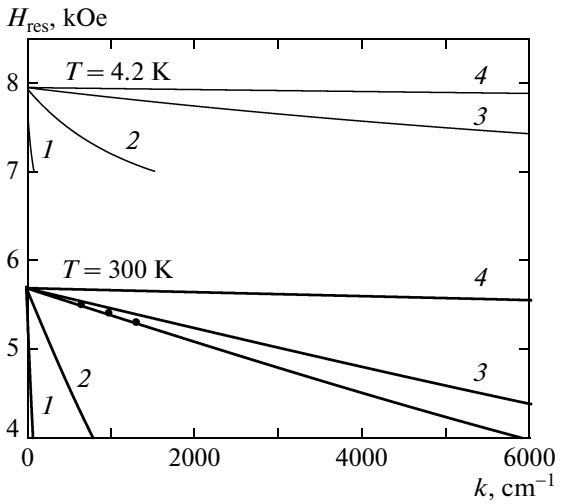

Fig. 7. Dispersion dependence $H_{res}(k)$ of a thin $CuCr_2S_4$ plate for various temperatures and plate thicknesses: $d = 10^{-2}$ (*1*), 10^{-3} (*2*), 10^{-4} (*3*), and 10^{-5} (*4*) cm. The dots indicate the positions of the experimental resonance fields for the first three magnetostatic oscillation modes.

Fig. 6. Electron microscope image of the investigated sample region.

spinel layers in this case is less than 0.1 μm. The situation where the $CuCr_2S_4$ plate does not reach the sample end is also possible.

To estimate the geometrical sizes of the $CuCr_2S_4$ plates, we calculated the dispersion dependence of the resonance fields for the magnetostatic modes on their wave vector, $H_{res}(k)$, shown in Fig. 7.

We fitted the data by the least-squares method by solving the equation for direct bulk magnetostatic waves propagating in an unbounded (in two dimensions) plane-parallel ferromagnetic plate [13] magnetized perpendicularly to its plane:

$$\tan\xi = \frac{2\xi/k_y d}{(\xi/k_y d) - 1},$$

where

$$\xi = \sqrt{-\mu}k_y d, \quad \mu = \frac{\omega_H\omega_H + \omega_M - \omega^2}{\omega_H^2 - \omega^2},$$

k_y is the wave vector, d is the plate thickness, $\omega_H = \gamma H_0 - \omega_M$, $\omega_M = 4\pi\gamma M_0$. The magnetostatic waves were assumed to be homogeneous in a direction perpendicular to the plate plane.

The following parameters give the closest coincidence between the theoretical dependence and experimental values: $k_y = 652.74$ cm^{-1} for the magnetostatic mode with $n = 2$ and $d = 1.35 \times 10^{-4}$ cm. Thus, adopting $n \cdot 2\pi/L = k$ for a plate of finite sizes, where L is the plate length, we have $L = 0.019$ cm.

Figure 8 shows the magnetic resonance spectra for two samples differing by the synthesis conditions (the transfer rate and concentration of the active agent). There are distinct differences in the spectra of magnetostatic oscillations for various samples. In our view, such differences can be associated with different geometrical sizes of the $CuCr_2S_4$ spinel layers. This suggests that the topology of the grown crystals is highly sensitive to their growth conditions.

An unusual behavior of the intensity of magnetostatic modes engages our attention. Under normal observation conditions, their intensity decreases with increasing distance from the homogeneous ferromagnetic resonance (the main line). In our case, the reverse is true (see Figs. 3 and 8).

In our opinion, this fact can be explained by the specificity of the microstructure of the investigated samples. We think (see Fig. 6) that the sample is a heterostructure where thin single-crystal $CuCr_2S_4$ regions are located between single-crystal $CuCrS_2$ layers. The $CuCrS_2$ layers in the investigated temperature range are paramagnetic ($T_N = 37$ K) with Cr^{3+} ($S = 3/2$). In an external magnetic field H_0, the Larmor precession frequency of such ions is $\omega_L = \gamma H_0$ and, in the case under consideration, coincides with or is very close to one of the boundary values of the domain of existence of magnetostatic modes (ω_0/γ). Thus, the $CuCr_2S_4$ layer is in an additional field oscillating with the frequency $\omega_L = \gamma H_0$ that modulates and amplifies the magnetostatic oscillation modes predominantly in the region of fields $\omega_0/\gamma = 3393$ Oe. To estimate the modulating field strength, we calculated the dipole field in the [001] direction produced by a $CuCrS_2$ layer with a size of $100 \times 100 \times 100$ lattice constants. The calcula-

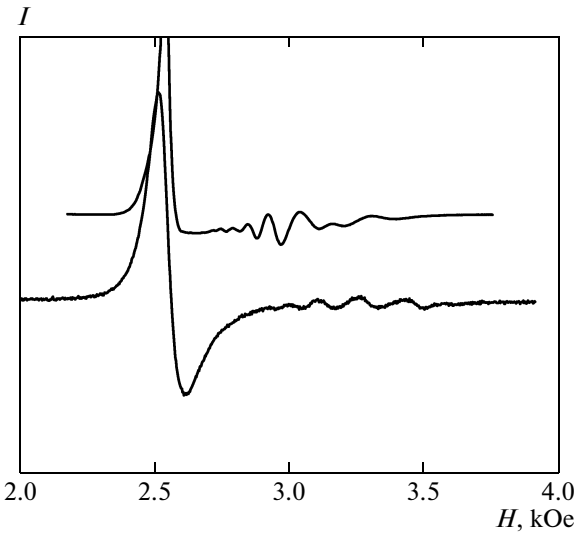

Fig. 8. Magnetic resonance spectra for two different samples of the Cu–Cr–S system. The external magnetic field is parallel to the plane of the plates.

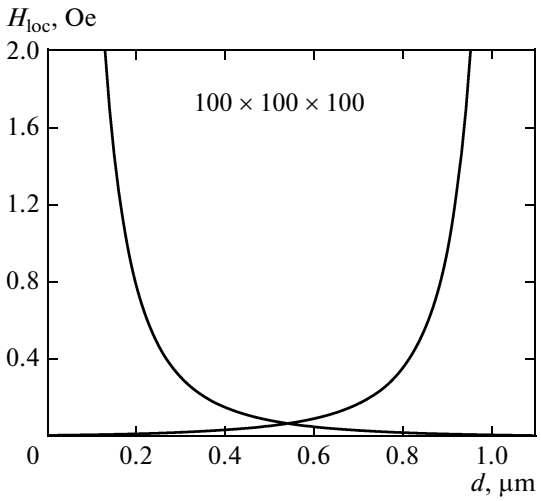

Fig. 9. Estimate of the modulating field distribution in a $CuCr_2S_4$ layer of thickness d located between single-crystal $CuCr_2S_4$ layers.

tions were performed for $T = 0$ K. The results are shown in Fig. 9.

Figure 9 shows a 1.1-μm-thick layer of the spinel phase with the $CuCrS_2$ phase located to the left and the right from it. The solid lines indicate the modulating field strength H_{loc}. To ascertain whether the dipole sums converged, we calculated the dipole field produced by $CuCrS_2$ layers with sizes of $10 \times 10 \times 10$, $50 \times 50 \times 50$, and $100 \times 100 \times 100$ lattice constants. We established that the difference of the dipole fields from the layers of $50 \times 50 \times 50$ and $100 \times 100 \times 100$ lattice constants was less than 1%.

It can be seen from Fig. 9 that the modulating field at the boundaries of the $CuCr_2S_4$ layer ($d = 0$ and 1.1 μm) is considerably larger than 2 Oe and decreases with increasing d almost to zero for $d > 0$ μm on the left and $d < 1.1$ μm on the right.

Thus, the bulk of the $CuCr_2S_4$ layer (0.2 μm $\le d \le$ 0.8 μm) is modulated by a total field with a strength of about 0.4 Oe. Consequently, the magnetostatic oscillation modes with $\omega \sim \omega_L$ are modulated much more strongly by the dipole fields from the $CuCrS_2$ layers, increasing their amplitude most dramatically in fields of ~3400 Oe.

In addition, in the region of intersection between the EPR branch of $CuCr_2S_4$ and the branch of magnetostatic oscillations, there are coupled oscillations that lead to repulsion and entanglement of the branches. It is most likely for this reason that the domains of existence of the magnetostatic oscillations for two field orientations intersect at low temperatures (see Fig. 5).

4. CONCLUSIONS

We grew single-crystal Cu–Cr–S samples that are single-crystal $CuCrS_2$ layers with thin spinel-phase ($CuCr_2S_4$) plates located among them. The Curie temperature ($T_C = 420$ K) and saturation magnetization of the spinel phase $CuCr_2S_4$ ($M_0 = 420$ G) were determined by the electron magnetic resonance method. The geometrical sizes of the $CuCr_2S_4$ plates and the wave vector of the magnetostatic oscillations in them were estimated. We found an anomalous behavior of the amplitude of magnetostatic oscillation modes in the $CuCr_2S_4$ plates attributable to their modulation by the Larmor precession of the magnetization of adjacent $CuCrS_2$ layers. We also established the dependence of the topology of the investigated crystals on synthesis conditions from sample to sample. A stricter control of the growth conditions and the choice of optimal parameters for the deposition of initial components will most likely allow one to control the thickness and distribution of the $CuCr_2S_4$ layers in a $CuCrS_2$ matrix and, consequently, to control the parameters of the spectra for the homogeneous ferromagnetic resonance and magnetostatic oscillations.

ACKNOWLEDGMENTS

This work was supported by the "New Nanosized and Layered Copper-Containing Sulfides for Electronics" International CRDF–Siberian Branch of the Russian Academy of Sciences grant for 2012 (RUP1-7054-KR-11, no. 16854).

REFERENCES

1. J. A. Wilson and A. D. Yoffe, Adv. Phys. **18**, 193 (1969).
2. J. Rouxel, A. Meershaut, and G. A. Wiegers, J. Alloys Compd. **229**, 144 (1995).
3. My. A. Boutbila, J. Rasneur, M. El. Aatmani, and H. Lyahyaoui, J. Alloys Compd. **244**, 23 (1969).

4. P. F. Bongers, C. F. van Bruggen, J. Koopstra, and W. P. A. M. Omloo, J. Phys. Chem. Solids **29**, 977 (1968).
5. M. Wintenberger and Y. Allain, Solid State Commun. **64**, 1343 (1987).
6. R. F. Almukhametov, R. A. Yakshibayev, E. V. Gabitov, and I. B. Ableev, Ionics **3**, 292 (1997).
7. G. M. Abramova, A. M. Vorotynov, G. A. Petrakovskiy, N. I. Kiselev, D. A. Velikanov, A. F. Bovina, R. F. Al'mukhametov, R. A. Yakshibaev, and E. V. Gabitov, Phys. Solid State **46** (12), 2225 (2004).
8. J. C. E. Rasch, M. Boehm, C. Ritter, H. Mutka, J. Schefer, L. Keller, G. M. Abramova, A. Cervellino, and J. F. Löffler, Phys. Rev. B: Condens. Matter **80**, 104431 (2009).
9. N. Le Nagard, G. Collin, and O. Gorochov, Mater. Res. Bull. **14**, 1411 (1979).
10. G. Abramova, G. Petrakovskiy, R. Szymczak, V. Sokolov, A. Vorotynov, D. Velikanov, Ju. Gerasimova, H. Szymczak, A. Bovina, and N. Kiselev, in *Proceedings of the International INTAS Workshop "New Layered 3d-Materials for Spintronics," Paul Scherrer Institute, Villigen, Switzerland\PSI, March 31–April 3, 2008*, Proceedings 08-01, ISSN 1019-6447, December, 2008, p. 12.
11. G. Abramova, A. Pankrats, G. Petrakovskii, J. C. E. Rasch, M. Boehm, A. Vorotynov, V. Tugarinov, R. Szumszak, A. Bovina, and V. Vasil'ev, J. Appl. Phys. **107**, 093914 (2010).
12. V. Tsurkan, J. Hemberger, A. Krimmel, H.-A. K. von Nidda, P. Lunkenheimer, S. Weber, V. Zestrea, and A. Loidl, Phys. Rev. B: Condens. Matter **73**, 224442 (2006).
13. A. G. Gurevich, *Magnetic Resonance in Ferrites and Antiferromagnets* (Nauka, Moscow, 1973) [in Russian].
14. A. A. Samokhvalov, Yu. N. Morozov, B. V. Karpenko, and M. I. Simonova, Phys. Status Solidi B **73**, 455 (1976).

Translated by V. Astakhov